

Araştırma Makalesi / Research Article

Performance Comparison of PID and NARX Neural Network for Attitude Control of a Quadcopter UAV

Şahin Ekmel KARAKAYA^{1*}, Aytaç GÖREN^{2,3}

¹ Dokuz Eylül Üniversitesi, Fen Bilimleri Enstitüsü, Mekatronik Mühendisliği Anabilim Dalı, İzmir, Türkiye,
ORCID ID: <https://orcid.org/0000-0002-0545-5499>, ekmel.karakaya@ogr.deu.edu.tr

² Dokuz Eylül Üniversitesi, Mühendislik Fakültesi, Makine Mühendisliği Bölümü, İzmir, Türkiye,
ORCID ID: <https://orcid.org/0000-0002-7954-1816>, aytac.goren@deu.edu.tr

³ Laboratory of Innovative Technologies, Picardie Jules Verne University, Amiens, France,
ORCID ID: <https://orcid.org/0000-0002-7954-1816>, aytac.goren@u-picardie.fr

Geliş/ Recieved: 17.10.2021;

Kabul / Accepted: 29.12.2021

ABSTRACT: In this study, two different types of controllers have been designed and tested for altitude and motion control of an autonomous quadrotor to compare the control performance under the influence of parametric uncertainty and disturbances. The first controller is a proportional-integral-derivative (PID) controller which is a conventional linear controller. The closed-loop PID algorithms calculate the results of the system by using the error values that consist of the difference between the sensor values measured by the closed-loop feedback method and the reference inputs. The second method that has been used is artificial neural network (ANN) algorithms, which provide both advantages and convenience in defining and controlling linear systems and non-linear systems with the closed-loop feedback method used in PID. The most important feature of the ANN algorithms is their high performance as a result of training with different input values. Therefore, the ANN control system has been trained with the input data used with Gaussian noise and the desired target data. A dynamic time series non-linear autoregressive with Exogenous input (NARX) neural network has been chosen as an ANN controller because of the time-delayed backpropagation learning performance. In this study, PID, and NARX NN control algorithms to control the maneuvers and altitude of the quadcopter and the mathematical model have been designed on Matlab Simulink. Motion control performances of the PID and NARX controllers are tested on the model. The design was tested on a real-time simulation environment with a one-millisecond fixed-step size. This paper proposes an alternative approach to control attitude and altitude on a quadcopter with the NARX NN algorithm.

Keywords: Attitude and altitude control, Quadcopter, Proportional-integrator-derivative, Non-linear autoregressive with external (Exogenous) input artificial neural networks, Gaussian noise.

*Sorumlu yazar / Corresponding author: ekmel.karakaya@ogr.deu.edu.tr

Bu makaleye atıf yapmak için / To cite this article

Karakaya, Ş. E., Gören, A. (2022). Performance Comparison of PID and NARX Neural Network for Attitude Control of a Quadcopter UAV. Journal of Materials and Mechatronics: A (JournalMM), 3(1), 1-19.

1. INTRODUCTION

The Newton-Euler equations and the Euler-Lagrange equations are the most common methods for aerial vehicles to build a mathematical model (Yoon et al., 2016; Paiva et al., 2016; Teppo Luukkonen, 2011; Wang et al., 2016; Hamidi et al., 2019; Nguyen et al., 2021; Muliadi and Kusumoputro, 2018; Praveen and Pillai, 2016; Cedro and Wieczorkowski, 2019; Razmi and Afshinfar, 2019). In addition, there is a study in the literature on dynamic system modeling of the quadcopter with dynamic time series non-linear autoregressive with Exogenous input (NARX) neural network (NN) (EIDakrory and Tawfik, 2016).

In the attitude and position controls of quadcopters, linear and non-linear system control is performed with optimal control, adaptive control, robust control, sliding control, proportional-integral-derivative (PID) control, artificial intelligence control methods (Zulu and John, 2014). Control systems need healthy and reliable position and behavior information generated by sensors to give reliable outcomes (Akin et al., 2021). The most widely used control system in quadcopters is the PID control system because of its easy implementation and adjustment (Cedro and Wieczorkowski, 2019; Praveen and Pillai, 2016; Muliadi and Kusumoputro, 2018; Wang et al., 2016; Yoon et al., 2016; Paiva et al., 2016; Luukkonen, 2011). In addition, there are studies of sliding control (Razmi and Afshinfar, 2019), fuzzy logic control (Hamidi et al., 2019), and dynamic PID coefficients update with direct inverse control (DIC) for attitude and altitude control (Muliadi and Kusumoputro, 2018) in the literature.

The quadcopter model is a non-linear dynamic system. Therefore, the non-linear system analysis feature of ANN algorithms will be advantageous in controlling the attitude and altitude of the quadcopter. The adaptive control performance of the NARX neural network, non-linear autoregressive moving average (NARMA-L2), and feedforward neural network (FFNN) structures from ANN algorithms on non-linear dynamic systems perform similar to each other (Hamidi et al., 2020). Conversely, NARX ANN has been used to predict future loads to increase performance for short-term forecasting of electric loads (Buitrago and Asfour, 2017). The NARX NN algorithm is one of the most promising methods to make predictions about the upcoming data to reach the optimal solution. Additionally, the NARX NN algorithm predicts the next value by checking the regressed previous values of the output signal and previous values of an exogenous input signal. The NARX NN algorithm can be used on many applications such as predictor, non-linear filtering, non-linear dynamic system modeling (Anonymous, 2021). ANN performance increases with random and different training data. The Gaussian noise time series are used to produce different training inputs for the NARX NN. In the literature, there are studies on the performance of neural network regression algorithms with Gaussian noise on ANN (Hagiwara et al., 2001) and non-linear dynamic system modeling with Gaussian process NARX (Tadej et al., 2021). Also, the Levenberg-Marquardt algorithm is used to train feedforward networks with increased performance results (Hagan and Menhaj, 1994). The planned attitude and altitude maneuvers have been diversified with smooth sinusoidal inputs and step inputs to observe the overshoot and steady-state responses of the system (Luukkonen, 2011; Yoon et al., 2016; Wang et al., 2016; Hamidi et al., 2019; Nguyen et al., 2021; Hamidi et al., 2020; Razmi and Afshinfar, 2019). Therefore, sinusoidal wave, sawtooth wave, and square wave have been used in this study.

This paper focused on the creation of the simulation environment and control algorithms were designed with the help of Simmechanics and mathematical models. PID control algorithms were found by the experimental Ziegler-Nichols method. NARX NN control was chosen because of its multi-step prediction feature in closed-loop and open-loop systems. Therefore, NARX NN to give

high performance, neural network training was realized by giving sinusoidal, sawtooth, square inputs, and Gaussian noise sequence input data. The trained NARX NN and PID controls of model roll, pitch, yaw, and altitude are tested on a real-time Matlab Simulink environment to compare their performances.

2. MODELLING

The mathematical model of roll, pitch, yaw, and x, y, z displacements of the quadcopter has been generated with the Newton-Euler and Euler-Lagrange equations. In the aerospace industry, inertial frame and body frame have been used to define the motions of the vehicle. Accordingly, these frames have been used to define the attitude and altitude of the quadcopter. The position vector is defined with $\xi = [x \ y \ z]^T$, roll, pitch, yaw equations defined with $\eta = [\phi \ \theta \ \psi]^T$ on the inertial frame. The linear velocity is defined with $Y = [u \ v \ w]^T$, the angular velocity defined with $\Omega = [p \ q \ r]^T$ on the body frame. The velocity of the quadcopter is shown in Equation 1, with the relation of rotational matrix Equation 4. Correspondingly the angular velocity of the quadcopter is shown in Equation 2, with the relation of angular velocity transformation matrix Equation 3. Therefore, inertial and body frames are shown in Figure 1. (Nguyen et al., 2021; Luukkonen, 2011; Hamidi et al., 2019; Wang et al., 2016; Razmi and Afshinfar, 2019; Paiva et al., 2016; Cedro and Wiczorkowski, 2019; Muliadi and Kusumoputro, 2018).

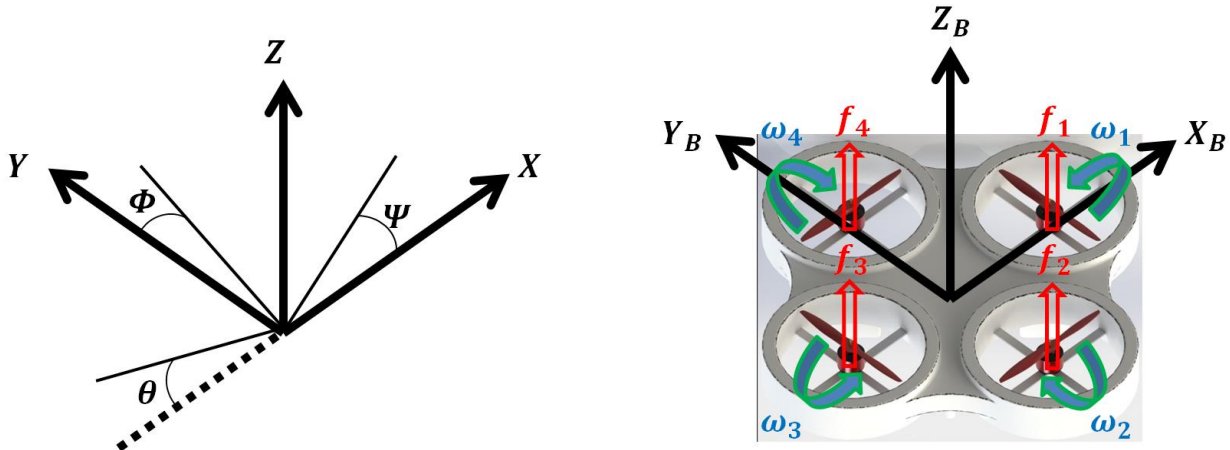


Figure 1. The inertial and body frames of the quadcopter

$$\dot{\xi} = RY \quad (1)$$

$$\dot{\eta} = J\Omega \quad (2)$$

$$J = \begin{bmatrix} 1 & 0 & -\sin\theta \\ 0 & \cos\phi & \sin\phi\cos\theta \\ 0 & -\sin\phi & \cos\phi\cos\theta \end{bmatrix} \quad (3)$$

$$R = \begin{bmatrix} \cos\theta\cos\psi & \cos\psi\sin\theta\sin\phi - \sin\psi\cos\phi & \cos\psi\sin\theta\cos\phi + \sin\psi\sin\phi \\ \cos\theta\sin\psi & \sin\psi\sin\theta\sin\phi + \cos\psi\cos\phi & \sin\psi\sin\theta\cos\phi - \cos\psi\sin\phi \\ -\sin\theta & \cos\theta\sin\phi & \cos\theta\cos\phi \end{bmatrix} \quad (4)$$

The lifting force and moments are defined in Equation 5 and Equation 6 where the k_f is the force constant, and k_m is the moment constant. In these equations, the effect of wing area has been selected as a constant. The total thrust and torque equations have been derived with the help of

Equation 5 and Equation 6 to achieve the roll, pitch, yaw, and altitude motions. As can be seen, the altitude maneuver is shown in Equation 7, the roll maneuver is shown in Equation 8, the pitch maneuver is shown in Equation 9, and the yaw maneuver is shown in Equation 10. (Nguyen et al., 2021; Luukkonen, 2011; Hamidi et al., 2019; Wang et al., 2016; Razmi and Afshinfar, 2019; Paiva et al., 2016; Cedro and Wiczorkowski, 2019; Muliadi and Kusumoputro, 2018).

$$f_i = k_f \omega_i^2 \quad (5)$$

$$\tau_i = k_m \omega_i^2 \quad (6)$$

$$T = k_f [\omega_1^2 + \omega_2^2 + \omega_3^2 + \omega_4^2] \quad (7)$$

$$\tau_\phi = lk_f [(\omega_2^2 + \omega_3^2) - (\omega_1^2 + \omega_4^2)] \quad (8)$$

$$\tau_\theta = lk_f [(\omega_1^2 + \omega_2^2) - (\omega_3^2 + \omega_4^2)] \quad (9)$$

$$\tau_\psi = k_m [(\omega_1^2 + \omega_3^2) - (\omega_2^2 + \omega_4^2)] \quad (10)$$

The rotational motion equations have been derived with the help of the Newton-Euler method. Two assumptions are made to simplify the equations. The first one is the symmetric quadrotor design and the second one is the center of the body frame intersecting with the center of gravity. Since these assumptions have been made diagonal inertia matrix of the quadcopter is shown in Equation 12. The rotational accelerations have been obtained with the help of Equation 11 and expressed in Equation 13 where roll acceleration is shown in Equation 14, pitch acceleration is shown in Equation 14, and yaw acceleration is shown in Equation 16. (Nguyen et al., 2021; Luukkonen, 2011; Hamidi et al., 2019; Wang et al., 2016; Razmi and Afshinfar, 2019; Paiva et al., 2016; Cedro and Wiczorkowski, 2019; Muliadi and Kusumoputro, 2018).

$$\begin{bmatrix} \tau_\phi \\ \tau_\theta \\ \tau_\psi \end{bmatrix} = I \ddot{n} + \times I \dot{n} \quad (11)$$

$$I = \begin{bmatrix} I_{xx} & 0 & 0 \\ 0 & I_{yy} & 0 \\ 0 & 0 & I_{zz} \end{bmatrix} \quad (12)$$

$$\begin{bmatrix} \tau_\phi \\ \tau_\theta \\ \tau_\psi \end{bmatrix} = \begin{bmatrix} I_{xx} \ddot{\phi} \\ I_{yy} \ddot{\theta} \\ I_{zz} \ddot{\psi} \end{bmatrix} + \begin{bmatrix} \dot{\theta} I_{zz} \dot{\psi} - \dot{\psi} I_{yy} \dot{\theta} \\ \dot{\psi} I_{xx} \dot{\phi} - \dot{\phi} I_{zz} \dot{\psi} \\ \dot{\phi} I_{yy} \dot{\theta} - \dot{\theta} I_{xx} \dot{\phi} \end{bmatrix} \quad (13)$$

$$\ddot{\phi} = \frac{\tau_\phi}{I_{xx}} + \frac{I_{yy}}{I_{xx}} \dot{\theta} \dot{\psi} - \frac{I_{zz}}{I_{xx}} \dot{\theta} \dot{\psi} \quad (14)$$

$$\ddot{\theta} = \frac{\tau_\theta}{I_{yy}} + \frac{I_{zz}}{I_{yy}} \dot{\psi} \dot{\phi} - \frac{I_{xx}}{I_{yy}} \dot{\psi} \dot{\phi} \quad (15)$$

$$\ddot{\psi} = \frac{\tau_\psi}{I_{zz}} + \frac{I_{xx}}{I_{zz}} \dot{\phi} \dot{\theta} - \frac{I_{yy}}{I_{zz}} \dot{\phi} \dot{\theta} \quad (16)$$

The translational motion equations are derived with the help of the Newton-Euler method and Newton's Second Law. Therefore $F = m \cdot a$ transformation of the quadcopter is shown in Equation 17. The x, y, z dimensional accelerations are shown in Equation 18, Equation 19, and Equation 20. (Nguyen et al., 2021; Luukkonen, 2011; Hamidi et al., 2019; Wang et al., 2016; Razmi and Afshinfar, 2019; Paiva et al., 2016; Cedro and Wiczorkowski, 2019; Muliadi and Kusumoputro, 2018).

$$m\ddot{\xi} = \begin{bmatrix} 0 \\ 0 \\ mg \end{bmatrix} + R \begin{bmatrix} 0 \\ 0 \\ -T \end{bmatrix} \quad (17)$$

$$\ddot{x} = \frac{-T}{m} (\sin\phi\sin\psi + \cos\phi\cos\psi\sin\theta) \quad (18)$$

$$\ddot{y} = \frac{-T}{m} (\cos\phi\sin\psi\sin\theta - \cos\psi\sin\phi) \quad (19)$$

$$\ddot{z} = g - \frac{T}{m} (\cos\phi\cos\theta) \quad (20)$$

The attitude and altitude of the quadcopter have been controlled with the help of the PID algorithm, and NARX NN algorithm. The subtraction of sensor value from reference input has been used to generate the error value (E_s) for the attitude and altitude maneuvers. These error values of the attitude and altitude have been used with the generic PID algorithm Equation 21, and the generic trained NARX NN algorithm Equation 22. The abbreviations used in Equation 21 and Equation 22 are P is the proportional coefficient, I is the integral coefficient, D is the derivative coefficient, N is the filter coefficient, $y(t)$ is the predict time series of NARX NN, $x(t)$ is the input time series of the NARX NN, d is the past values of the $y(t)$. NARX NN algorithm has been trained with Levenberg-Marquardt algorithm that shown in Equation 23. It follows that the training algorithm uses the Hessian matrix with Newton's method where J^T is the transpose of the Jacobian matrix, J is the Jacobian matrix, I is the identity matrix, μ is the editible variable, e is all errors, and x is the weight and bias variables. Levenberg-Marquardt algorithm decreases μ after each successful step and increased only with tentative step in order to increase performance at each iteration of the algorithm. NARX NN architecture is shown in Figure 2. (Buitrago and Asfour, 2017; Hagan and Menhaj, 1994; Anonymous, 2021).

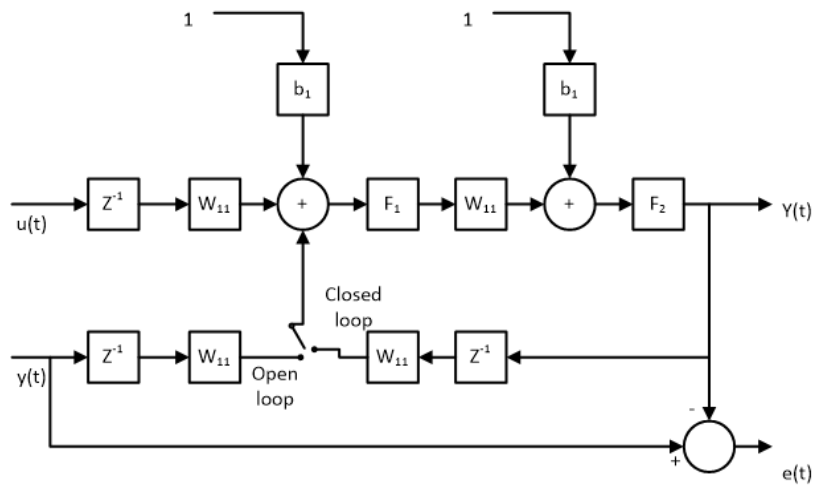


Figure 2. The NARX NN architecture. (Buitrago and Asfour, 2017)

$$PID_s = E_s P + E_s I \frac{1}{s} + E_s D \frac{N}{1 + N \frac{1}{s}} \quad (21)$$

$$y(t) = f(x(t-1), \dots, x(t-d), y(t-1), \dots, y(t-d)) \quad (22)$$

$$\Delta x = x_{k+1} - x_k = [J^T J + \mu I]^{-1} J^T e \quad (23)$$

3. METHODOLOGY

In this study, a closed-loop feedback system has been used in the control methodology. The subtraction of sensor value from reference input has been used to generate the error value E_s for the attitude and altitude maneuvers. These error values of the attitude and altitude have been used with the generic PID algorithm is shown in Equation 21, and the generic NARX NN algorithm is shown in Equation 22. The reference inputs and sensor outputs are meters for altitude, and degree for roll, pitch, and yaw. The outputs of the PIDs are summarized with the help of Equation 7, Equation 8, Equation 9, and Equation 10 to generate desired rotor commands. However, the trained NARX NN algorithm is replaced with the control blocks. The control system for the attitude and altitude of the quadcopter is shown in Figure 3.

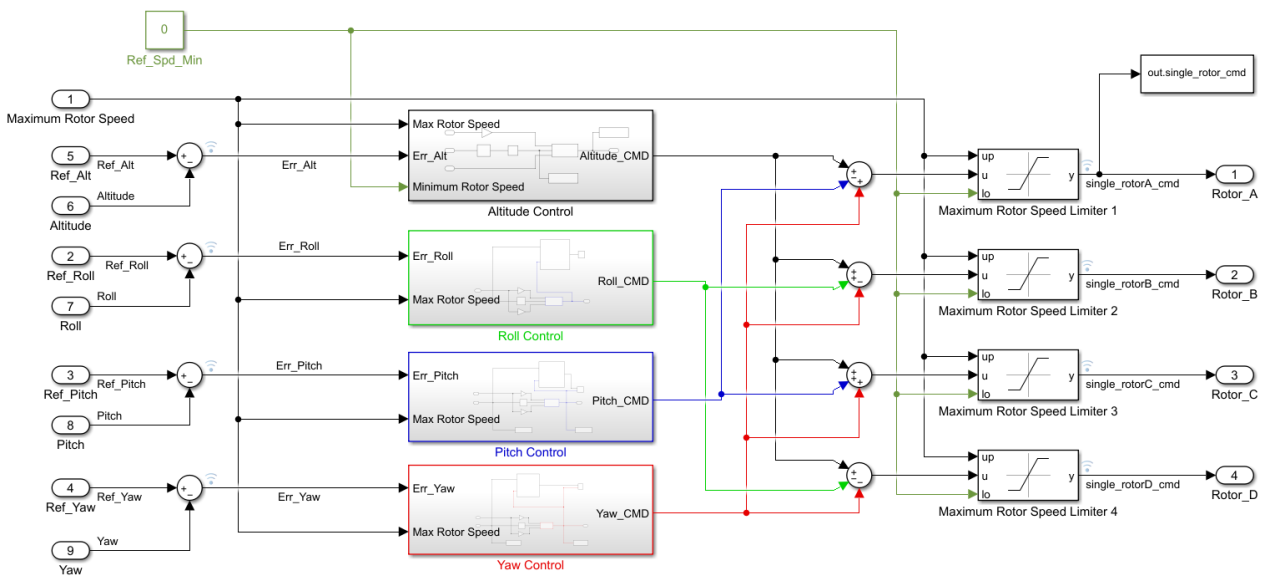


Figure 3. The control command generation for each rotor scheme for attitude and altitude of the quadcopter

4. SIMULATION

The simulation of the quadcopter has been modeled on the Matlab Simulink with the help of the Simscape blocks. The quadcopter model has been designed with four main subsystems that are shown in Figure 4. The reference inputs have been generated with the signal builder in the Reference Inputs block for the altitude in meters, and the attitude maneuvers in degree. The error values for the altitude and attitude have been calculated with the subtraction reference input from sensor outputs. Moreover, the four-rotor commands have been generated with PID or NARX NN control algorithms that have been supplied with the calculated error values in the Controller block. The dynamic and mathematical model of the voltage source, H-Bridge, rotors, propellers, and the body-frame of the 3D quadcopter model have been designed under the QuadCopter block. The properties of mass and construction of quadcopter have been calculated with the help of Solidworks. The distance between the quadcopter and the motors “ l ” has been used to define the angular velocities and resultant forces acting on the rotors shown in Figure 1. The quadcopter design has been designed counterpoised dimensional axis. Since the relation of quadcopter and altitude, and maneuvers are shown in Equation 14,15,16,18,19,20. The total quadcopter mass “ m ”, and mass moment of inertia about x, y, z axis “ I_{xx}, I_{yy}, I_{zz} ” has been used on Quadcopter block with SimMechanics blocks to create a mathematical model of the quadcopter. The quaternions, the world-frame, sensor values of the

attitude and altitude have been calculated under the Sensor Calculations block. The gravitational acceleration g has been used on the World frame in the Sensor Calculations subsystem to make a relation between environment and quadcopter. Solidworks have been used to design the 3D model of the quadcopter and calculate the weight and inertias. The design parameters are shown in Table 1.

Table 1. The design parameters

Name	Symbol	Value	Name	Symbol	Value
Total Mass	m	2.822 kg	Mass moment of inertia about x -axis	I_{xx}	1.93 kgm ²
Gravity	g	9.81 ms ⁻²	Mass moment of inertia about y -axis	I_{yy}	1.96 kgm ²
Distance between the quadcopter center and the motors	l	0.282 m	Mass moment of inertia about z -axis	I_{zz}	0.27 kgm ²

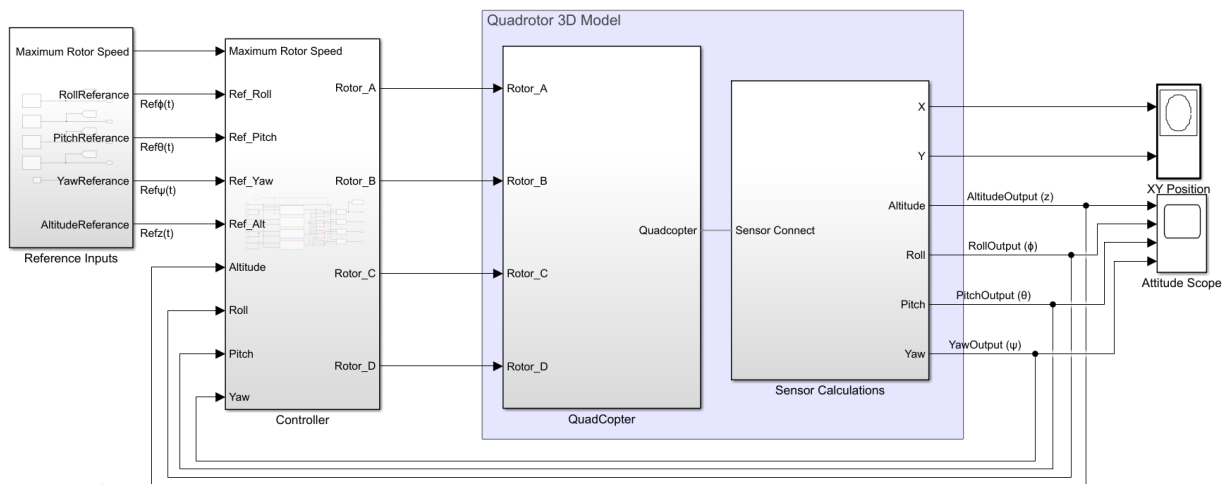


Figure 4. The control command generation for each rotor scheme for attitude and altitude of the quadcopter

The attitude and altitude commands have been calculated inside the controller block. The altitude command has been limited with 0.8 of the maximum total rotor speed. Correspondingly, roll, pitch, and yaw maneuvers are limited with 0.1 of the maximum total rotor speed. The PID controller has been used to set overshoot between %5-9 range and to set steady-state response between 6 seconds. Therefore, the PID controller coefficients have been found with the Ziegler- Nichols method. As described, the general PID control scheme is shown in Figure 5.

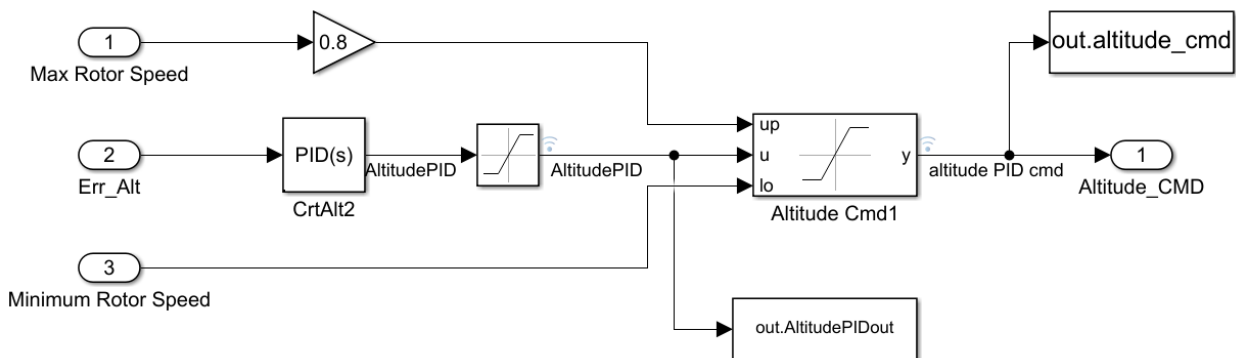


Figure 5. The schematic model of the PID control algorithm

The NARX NN algorithm has been used instead of the PID block and the saturation block. The schematic model of the NARX NN control is shown in Figure 6. The NARX neural network structure has trained with the sinusoidal wave, square wave, and Gaussian noise reference inputs and altitude commands as a target. A total of 300000 data has been used to train the network with the Levenberg-Marquardt algorithm. The altitude reference inputs that have been used to train the neural network are shown in Figure 7. The neural network with 25 neurons was trained for the altitude movement command. Likewise, the yaw maneuver has trained with the sinusoidal wave, square wave, sawtooth wave, and Gaussian noise reference inputs. The yaw reference inputs used to train NARX neural network is shown in Figure 8. The NARX neural network with 43 neurons has trained for the yaw maneuver command. Similarly, the roll and pitch maneuvers have been trained with the sinusoidal wave, square wave, sawtooth wave, and Gaussian noise reference inputs. The roll and pitch maneuver reference inputs used to train NARX neural network are shown in Figure 9. The NARX neural network with 64 neurons has been trained for the roll and pitch maneuver commands.

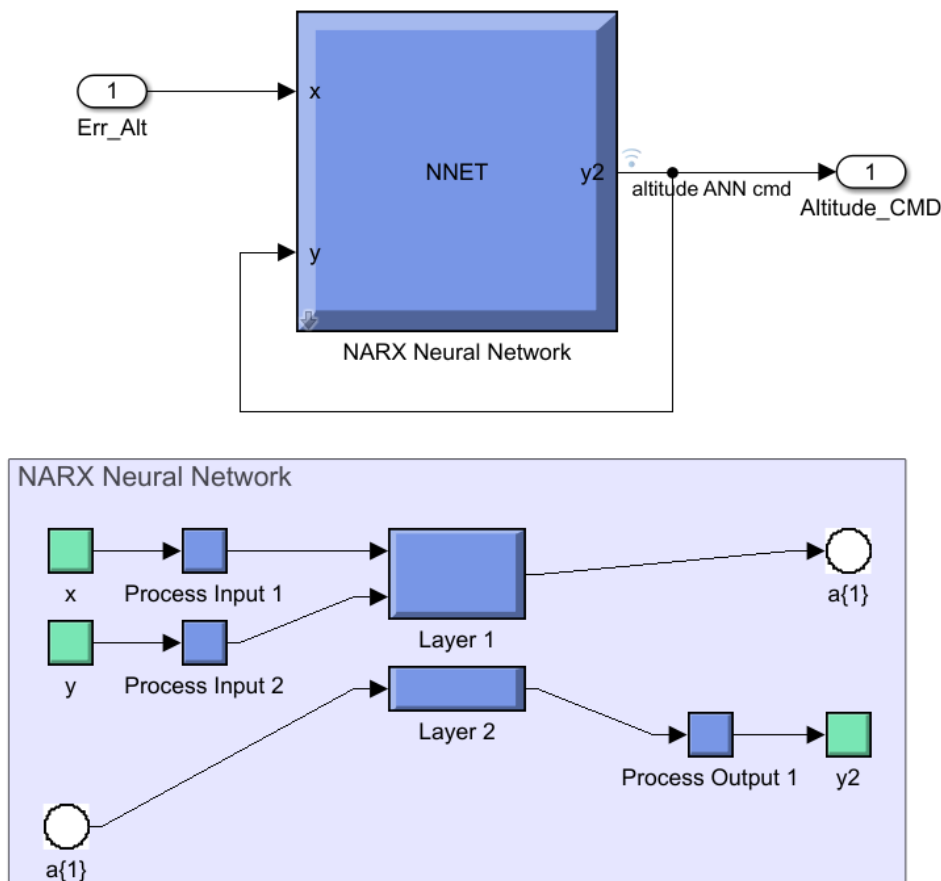


Figure 6. The schematic model of the NARX neural network

The altitude reference input has been set in three different signal types with Gaussian noise. The sine wave has been used between 0-100 seconds which is generated with 0.1 Hz frequency, 2.5 meters offset, and 1-meter amplitude. The square wave has been used between 100-200 seconds which is generated with the same frequency, offset, and amplitude. The random step input has been used between 200-300 seconds which is generated with 0.5 meters to 3 meters amplitude variation for 5 seconds. The random Gaussian noise sequence has been used between 0-300 seconds which is generated with 1 Hz frequency, 0.5 mean amplitude. The resultant inputs are shown in Figure 7.

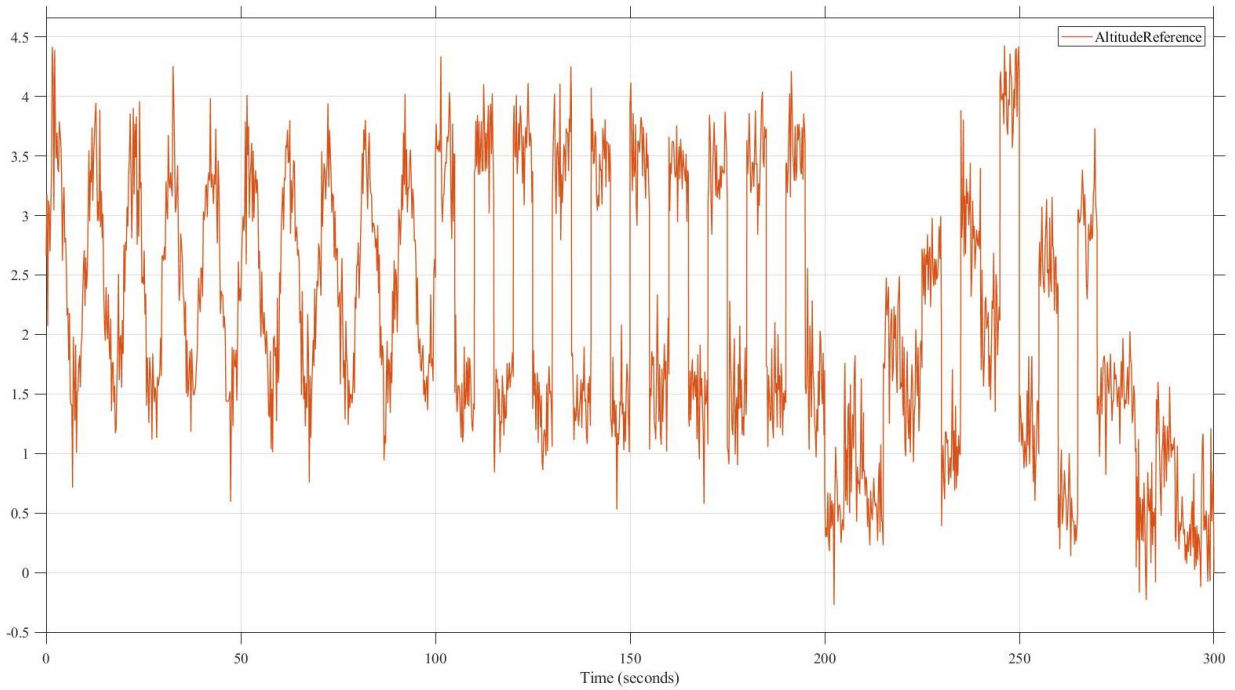


Figure 7. Altitude reference inputs used to train NARX neural network

The yaw reference input has been set in three different signal types with Gaussian noise. The sine wave has been used between 0-100 seconds which is generated with 0.5 Hz frequency with 20-degree amplitude. The square wave has been used between 100-200 seconds which is generated with 0.5 Hz frequency, 20-degree offset, and 20-degree amplitude. The sawtooth wave has been used between 200-300 seconds which is generated with the same frequency, offset, and amplitude of the square wave. The random Gaussian noise sequence has been used between 0-300 seconds which is generated with 1 Hz frequency, 0.5 mean amplitude. The resultant inputs for the yaw maneuver are shown in Figure 8.

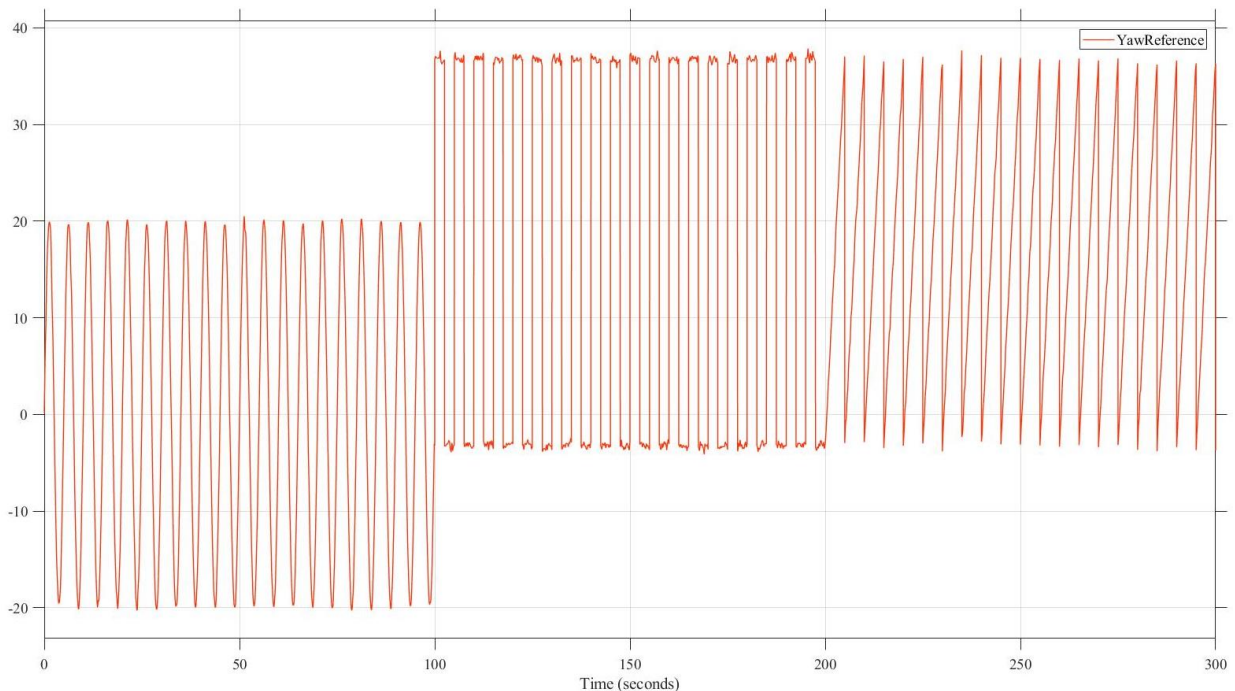


Figure 8. Yaw reference inputs used to train NARX neural network

The roll and pitch reference inputs have been set in three different signal types with Gaussian noise. The sine wave between 0-100 seconds, the square wave between 100-200 seconds, and the sawtooth wave between 200-300 seconds have been generated with 0.5 Hz frequency and 5-degree amplitude. The random Gaussian noise sequence has been used between 0-300 seconds which is generated with 1 Hz frequency, 0.5 mean amplitude. The resultant inputs for the roll and pitch maneuvers are shown in Figure 9.

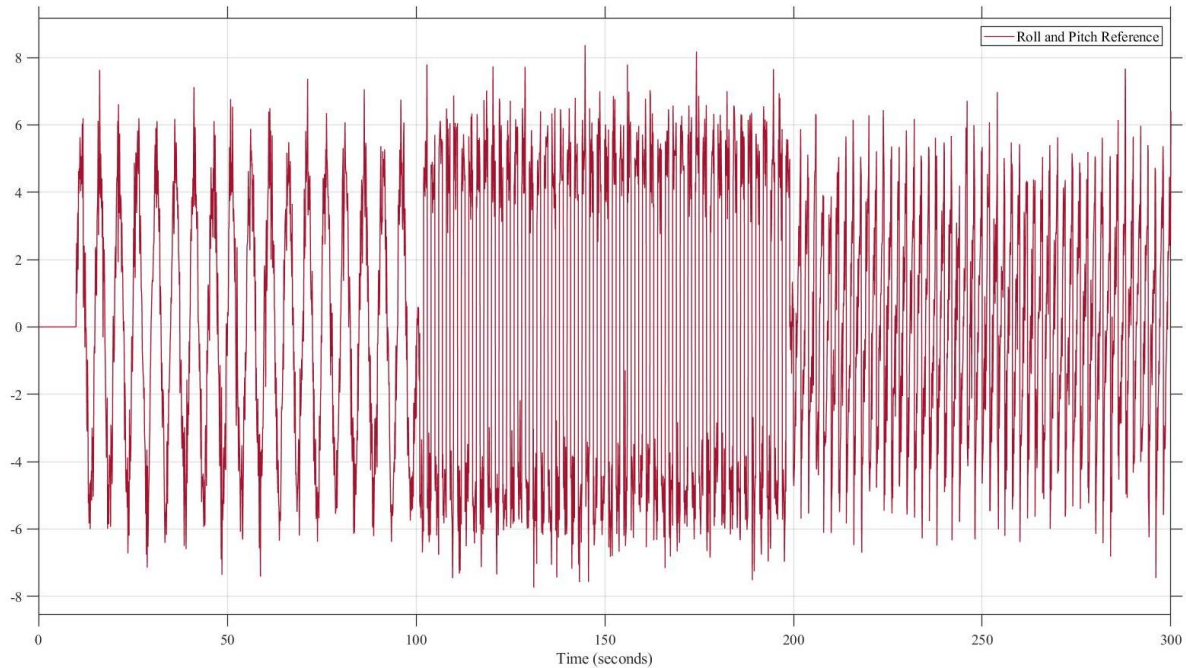


Figure 9. Pitch and roll reference inputs used to train NARX neural network

5. RESULTS AND DISCUSSION

The verification process of the model has been assisted with a 3-D simulation to improve the visualization of roll, pitch, yaw, and altitude maneuvers. The visual simulation has been run with the Simulink Mechanics Explorer application. The Simulink 3-D simulation environment is shown in Figure 10.

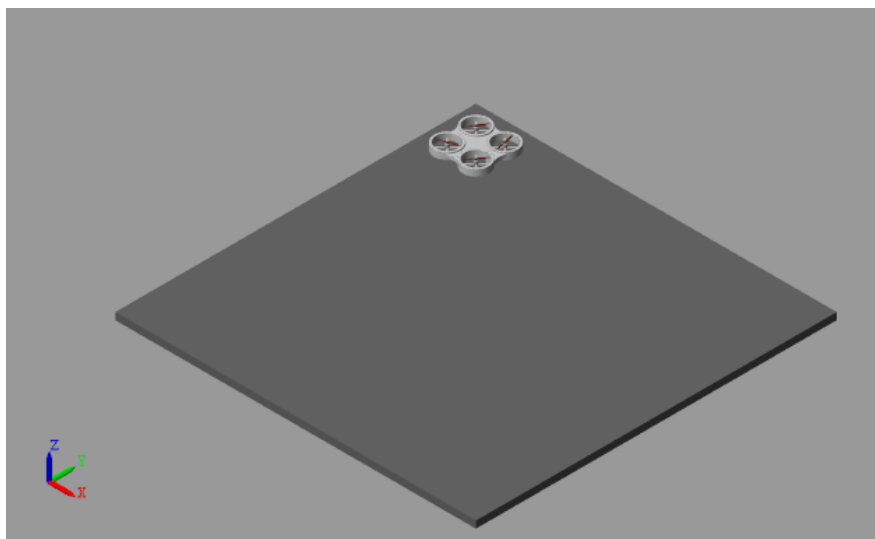


Figure 10. Matlab Mechanics Explorer simulation environment for the designed quadcopter.

The PID coefficients of the attitude and altitude maneuvers have been tuned with the Ziegler-Nichols method. The altitude, roll, and pitch PID coefficients have been set with classic Ziegler-Nichols coefficients shown in Equation 23 for the linearized quadcopter. The continuous oscillation has been found by assigning proportional gain to the system. The ultimate gain (K_u) has been set 80 for altitude and 3.8 for roll and pitch maneuvers. The oscillation period (T_u) has been found 1.83 for altitude and 0.92 for roll and pitch maneuvers. On the other hand, the yaw maneuver has been set with proportional gain. The results of the PID coefficients are shown in Table 2.

$$[K_p, K_i, K_d] = [0.6K_u, 1.2 \frac{K_u}{T_u}, 0.075K_u T_u] \quad (23)$$

Table 2. The PID coefficients for roll, pitch, yaw, altitude maneuvers

Maneuvers	Proportional (P)	Integral (I)	Derivative (D)	Filter Coefficient (N)
Altitude	48	52.459	10.98	100
Roll	2.28	4.9565	0.2622	100
Pitch	2.28	4.9565	0.2622	100
Yaw	6	0	0	250

The NARX NN algorithms have been trained with the Levenberg-Marquardt method in the Matlab Neural Network toolbox. The training inputs have been randomized with the help of random Gaussian numbers. The Gaussian number has been generated with 0.5 deviations on a 1 Hz frequency. The training state of attitude and altitude maneuvers with epoch numbers, Gradient, Mu, and Validation checks are shown in Figure 11 for altitude maneuver, Figure 12 for yaw maneuver, Figure 13 for pitch and roll maneuvers. As a result of training with the Levenberg-Marquardt method, the regression placement process results are shown in Figure 14 for altitude maneuver, Figure 15 for yaw maneuver, Figure 16 for pitch and roll maneuvers.

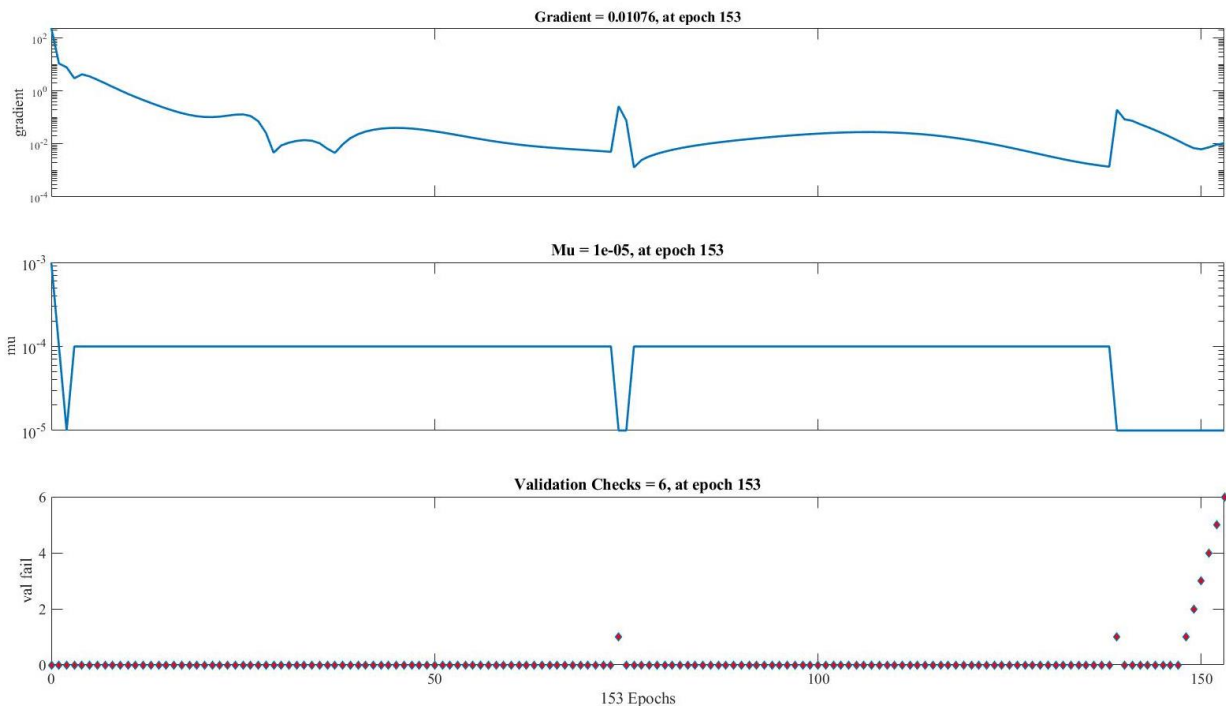


Figure 11. The training state data from ANN altitude training

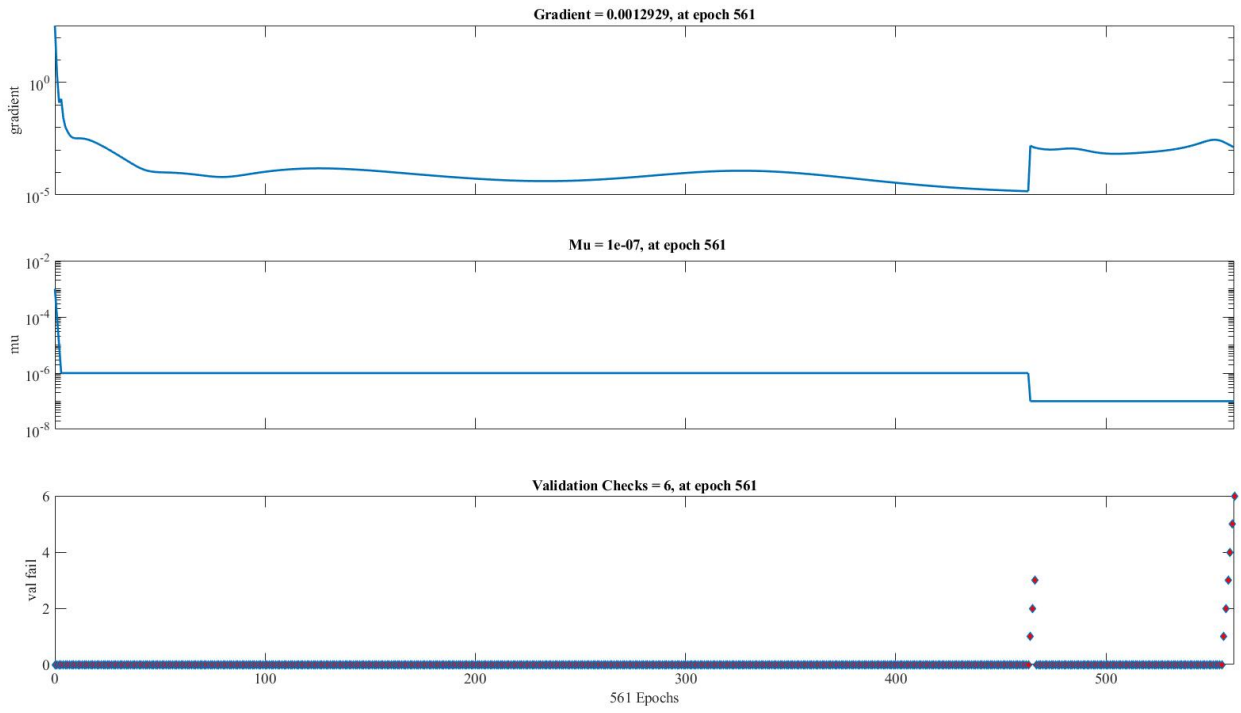


Figure 12. The training state data from ANN yaw training

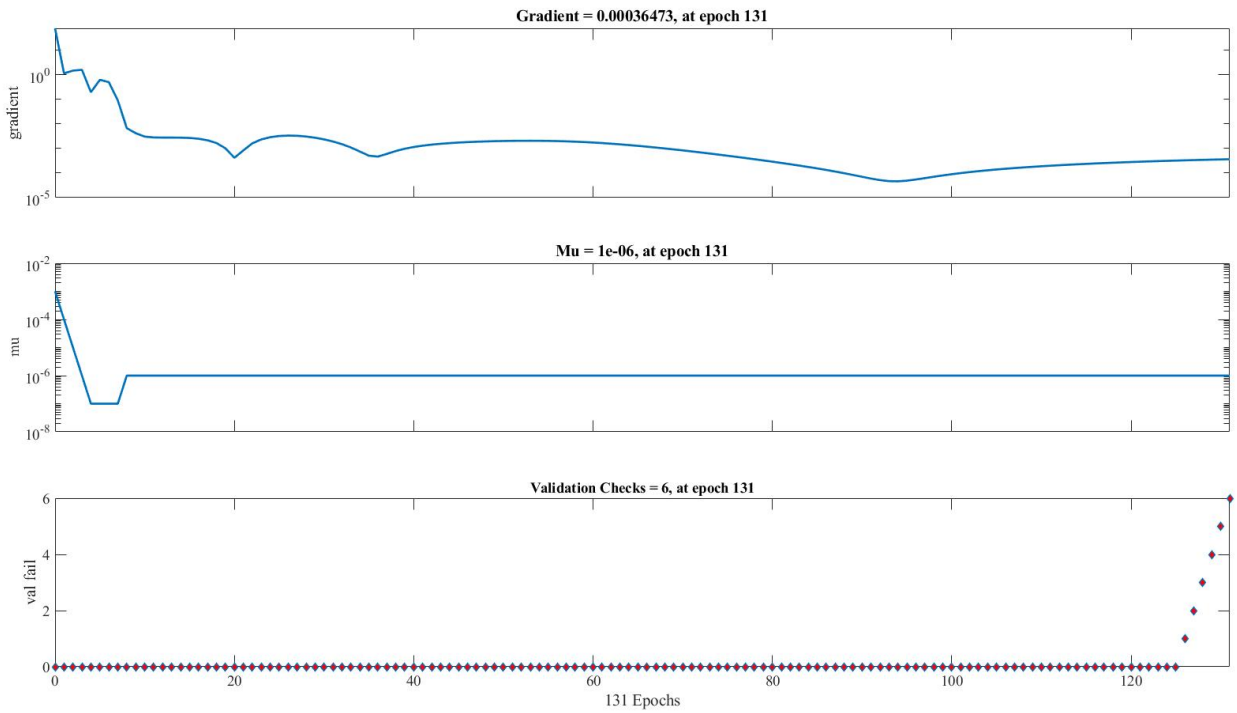


Figure 13. The training state data from ANN pitch and roll training

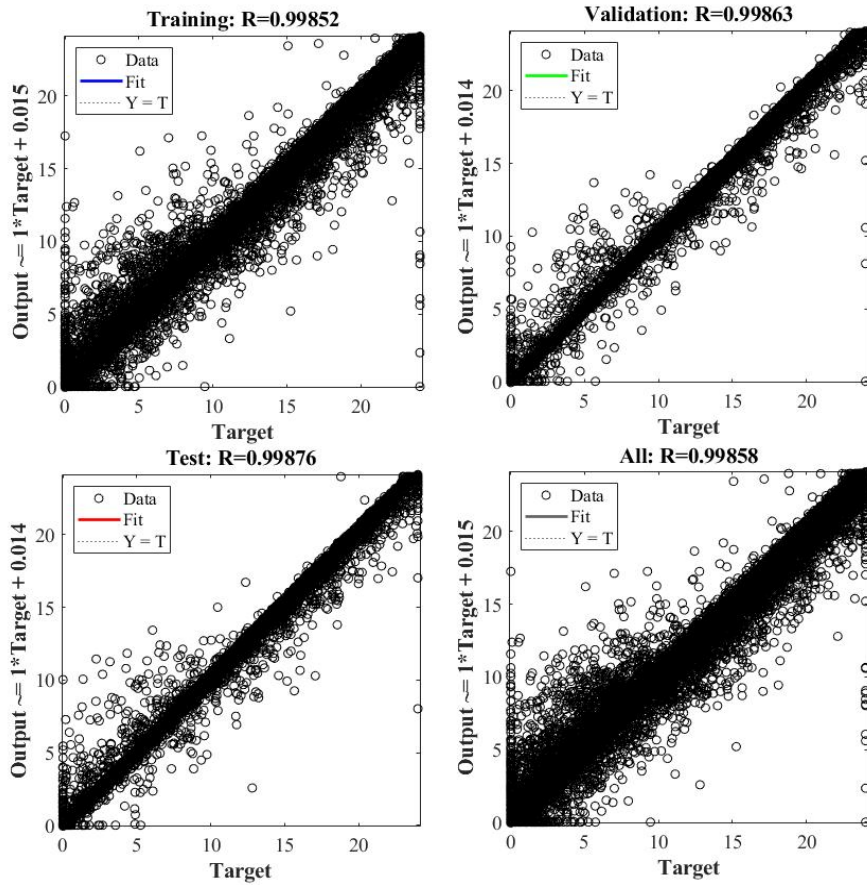


Figure 14. Regression results from ANN altitude training

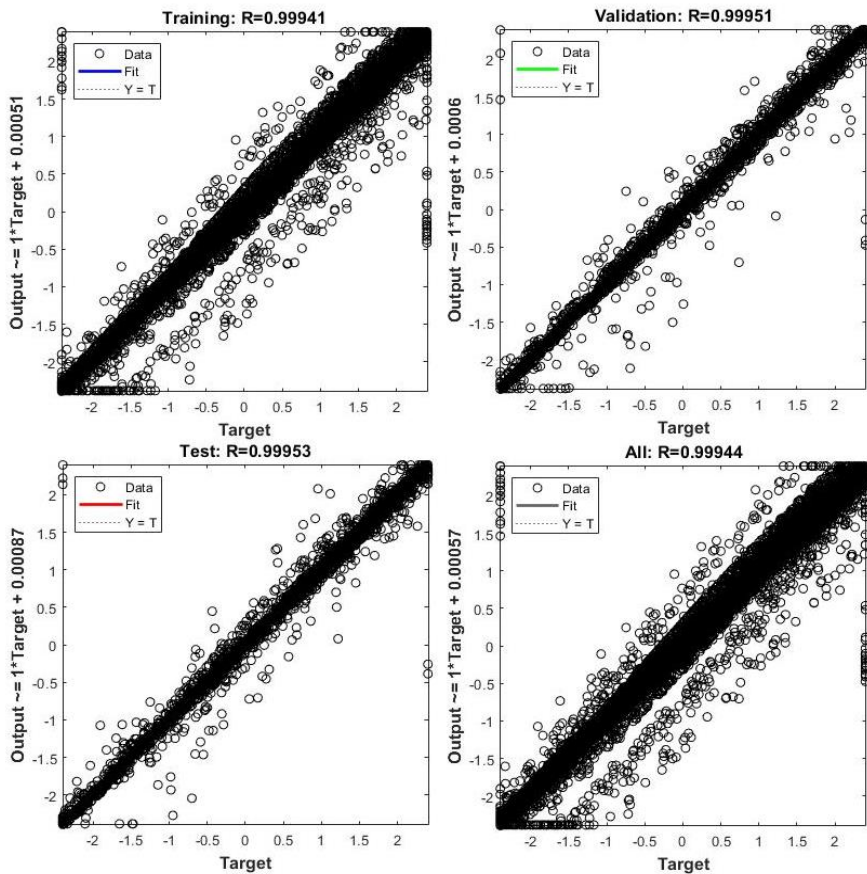


Figure 15. Regression results from ANN yaw training

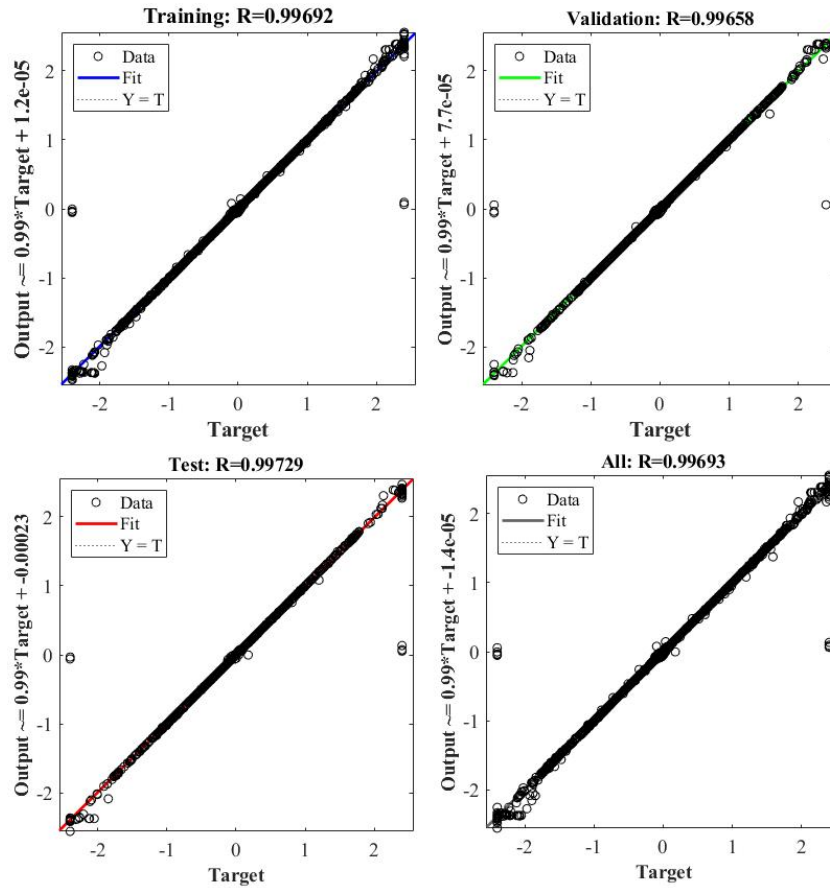


Figure 16. Regression results from ANN pitch and roll training

The PID and NARX NN algorithms have been designed and tested in five steps on the proposed quadcopter model shown in Figure 4. First, the mathematical model, environmental variables, and sensors have been designed. Second, the PID coefficients for each maneuver have been found with the Ziegler-Nichols method. Third, reference inputs that are shown in Figures 7,8,9, and desired outputs of the system have been generated with the help of the results of the PID algorithm for each maneuver. Fourth, the NARX NN algorithms for each maneuver have been trained by the Levenberg-Marquardt algorithm. Fifth, the Mean Square Error (MSE) and Root Mean Square Error (RMSE) have been calculated with both control algorithms for each maneuver. The results of PID control and NARX NN algorithms are compared under the sinusoidal wave, square wave, and sawtooth wave inputs without the Gaussian noise. The corresponding comparison of PID, NARX NN, and reference inputs are shown in Figure 17 for altitude maneuver, Figure 18 for yaw maneuver, Figure 19 for roll and pitch maneuvers. The performance comparison between the PID and NARX NN has been calculated with MSE and RMSE. The performance results are shown in Table 3.

Table 3. The performance results of attitude and altitude maneuvers

Error Type	Altitude (meter)	Roll (degree)	Pitch (degree)	Yaw (degree)
Mean Square Error (MSE) of NARX NN	0.137947	0.00277577	0.0264322	0.00512254
Root Mean Square Error (RMSE) of NARX NN	0.98523	0.996921	0.976153	0.999408
Mean Square Error (MSE) of PID Results	0.138773	0.01183	0.02668	0.01498
Root Mean Square Error (RMSE) PID Results	1.0273	0.99741	0.99954	0.99165

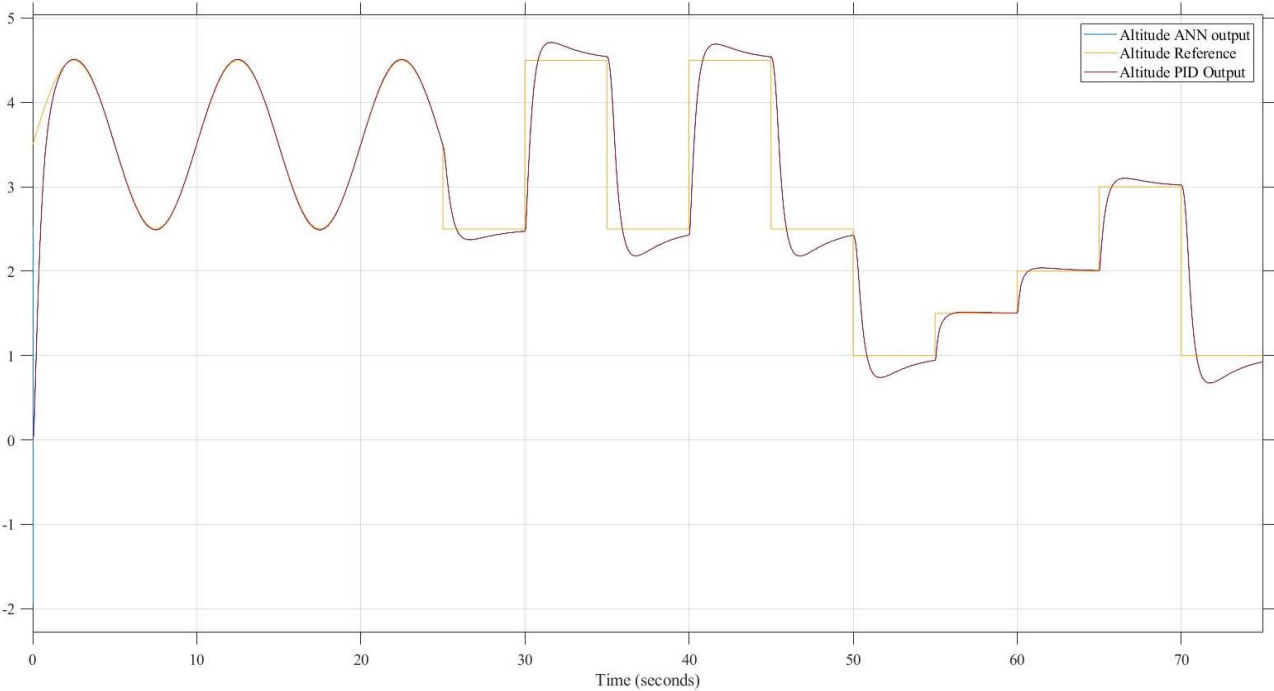


Figure 17. The comparison of the reference inputs, PID output, and ANN output for altitude

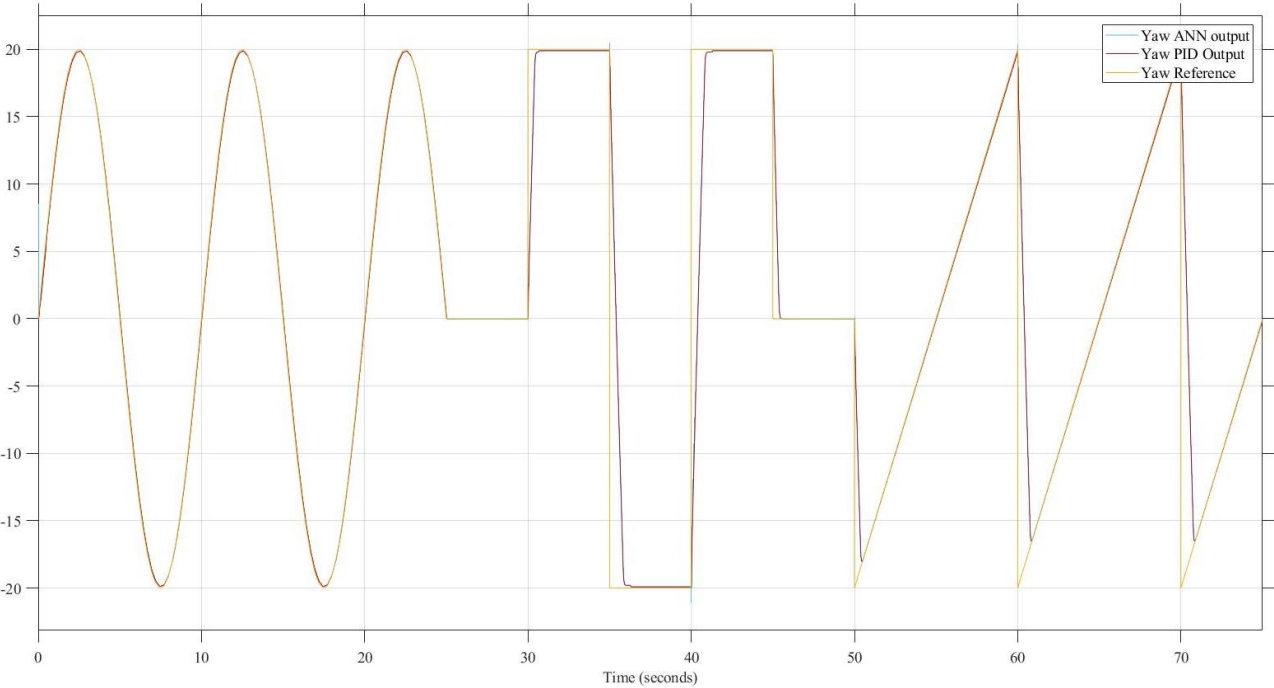


Figure 18. The comparison of the reference inputs, PID output, and ANN output for yaw

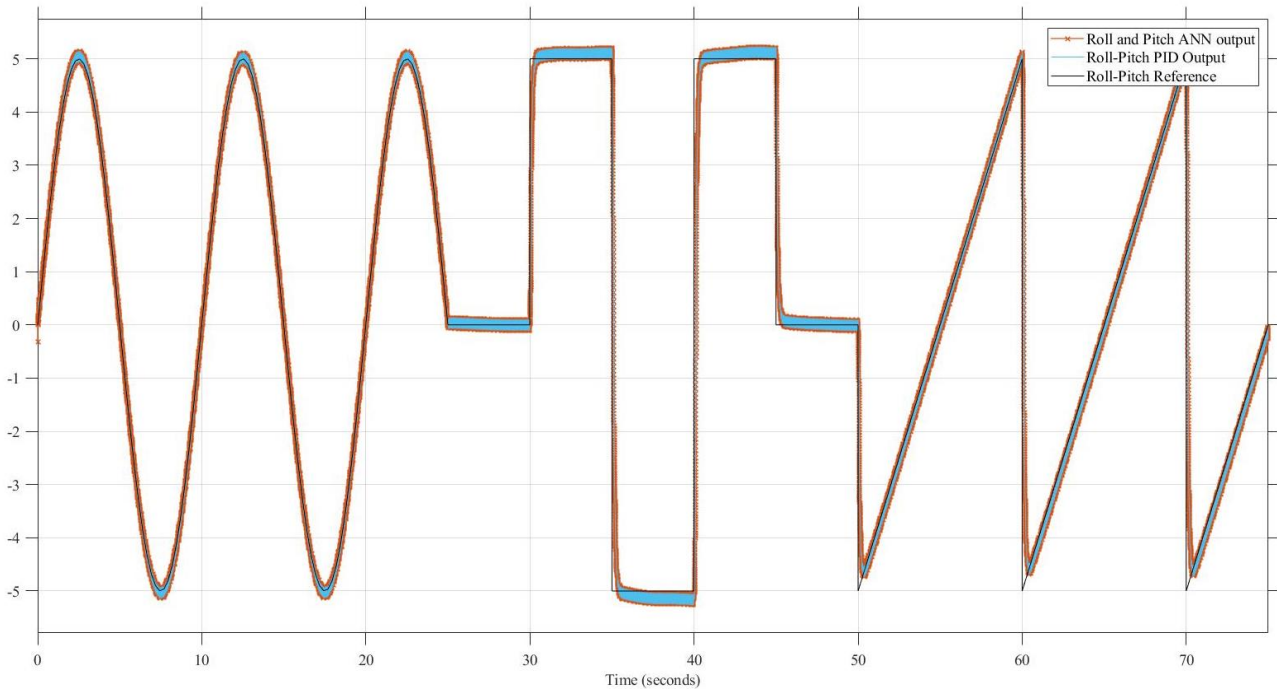


Figure 19. The comparison of the reference inputs, PID output, and ANN output for roll and pitch

6. CONCLUSION

This paper has been introduced the mathematical model of the quadcopter, and PID, NARX NN controller designs for the attitude and altitude maneuvers. Due to the non-linear analysis benefits of the NARX neural network algorithm, the trained data give similar results like the PID with a small amount of difference on RMSE and MSE errors. The NARX NN algorithm has performed better than the PID algorithm on controlling the attitude and altitude of the quadcopter. To clarify the results, the RMSE and MSE methods have been used. It follows that the altitude maneuver control by the NARX NN algorithm has given 0.98523 RMSE and 0.137947 MSE error where the PID algorithm 1.0273 RMSE and 0.138773 MSE error. Moreover, the roll maneuver control by the NARX NN algorithm has given 0.996921 RMSE and 0.00277577 error where the PID algorithm 0.99741 RMSE and 0.01183 MSE error. Likewise, the pitch maneuver control by the NARX NN algorithm has given 0.976153 RMSE and 0.0264322 MSE error where the PID algorithm 0.99954 RMSE and 0.02668 MSE error. However, the error values have given almost the same results on yaw maneuver control by NARX NN, and PID algorithm. The yaw maneuver control by the NARX NN algorithm has given 0.999404 RMSE and 0.00512254 error where the PID algorithm 0.99165 RMSE and 0.01498 MSE error. The most important criterion here is the multiplicity of training data used and training with different possibilities of inputs. In this way, the desired response can be obtained from the system under unexpected conditions. In real flights, when an accident or an undesired movement occurs, the response requested by the system can re-train the trained system with the data recorded during the flight to prevent future accidents.

7. CONFLICT OF INTEREST

Authors approve that to the best of their knowledge, there is not any conflict of interest or common interest with an institution/organization or a person that may affect the review process of the paper.

8. AUTHOR CONTRIBUTION

Şahin Ekmel KARAKAYA and Aytaç GÖREN contributed determining the concept and design process of the research and research management, data analysis and interpretation of the results, critical analysis of the intellectual content. Besides, Şahin Ekmel KARAKAYA contributed data collection, preparation of the manuscript, and final approval and full responsibility.

9. NOMENCLATURE

- ANN = Artificial Neural Network
- DIC = Direct Inverse Control
- FFNN = Feedforward Neural Network
- MSE = Mean Square Error
- NN = Neural Network
- NARMA-L2 = Non-linear Autoregressive Moving Average
- NARX = Non-linear Autoregressive with Exogenous Input
- PID = Proportional, Integral, Derivative
- RMSE = Root Mean Square Error
- UAV = Unmanned Aerial Vehicle
- $x = x$ Position
- $y = y$ Position
- $z = z$ Position
- Φ = Roll Angle
- Θ = Pitch Angle
- Ψ = Yaw Angle
- u = Linear Velocity on x -Axis
- v = Linear Velocity on y -Axis
- w = Linear Velocity on z -Axis
- p = Angular Velocity around x -Axis
- q = Angular Velocity around y -Axis
- r = Angular Velocity around z -Axis
- k_f = Force Constant
- k_m = Moment Constant
- I_{xx} = Mass Moment of Inertia About x -axis
- I_{yy} = Mass Moment of Inertia About y -axis
- I_{zz} = Mass Moment of Inertia About z -axis
- f_i = Lifting Force
- τ_i = Lifting Moment
- T = Altitude Maneuver Force
- τ_ϕ = Roll Maneuver Force
- τ_θ = Pitch Maneuver Force
- τ_ψ = Yaw Maneuver Force
- l = Distance Between the Quadcopter Center and the Motors

- ω_n = Angular Velocity of nth Rotor
- m = Total Mass of Quadcopter
- g = Gravitational Force
- E_s = Error Value
- N = Filter Coefficient
- K_u = Ultimate Gain
- T_u = Oscillation Period
- F = Force
- a = Acceleration

10. REFERENCES

- Akın M., Gören A., Rachid A., Implementation of Sensor Filters and Altitude Estimation of Unmanned Aerial Vehicle using Kalman Filter. *Journal of Mechatronics and Robotics* 5, 8-17, 2021.
- Anonymous, 2021, Mathworks Documentation, <https://www.mathworks.com/help/>.
- Buitrago J., Asfour S., Short-Term Forecasting of Electric Loads Using Nonlinear Autoregressive Artificial Neural Networks with Exogenous Vector Inputs. *Energies* 10(1):40, 1-25, 2017.
- Cedro L., Wiczorkowski K., Optimizing PID controller gains to model the performance of a quadcopter. *Transportation Research Procedia* 40, 156-169, 2019.
- El Dakrory A. M., Tawfik M., Identifying the Attitude of Dynamic Systems using Neural Network, 2016 International Workshop on Recent Advances in Robotics and Sensor Technology for Humanitarian Demining and Counter-IEDs (RST), 1-4, 2016.
- Hagan M., Menhaj M., Training Feedforward Networks with the Marquardt Algorithm, *IEEE Transactions on neural networks* 5(6), 989-993, 1994.
- Hagiwara K., Hayasaka T., Toda N., Usui S., Kuno K., Upper bound of the expected training error of neural network regression for a Gaussian noise sequence. *Neural Networks* 14(10), 1419-1429, 2001.
- Hamidi K. E., Mjahed M., Kari A. E., Ayad H., Adaptive Control Using Neural Networks and Approximate Models for Nonlinear Dynamic Systems. *Modelling and Simulation in Engineering* 2020:8642915, 1-13, 2020.
- Hamidi K. E., Mjaded M., Kari A. E., Ayad H., Neural Network and Fuzzy-logic-based Self-tuning PID Control for Quadcopter Path Tracking. *Studies in Informatics and Control* 28(4), 401-412, 2019.
- Krivec T., Papa G., Kocijan J., Simulation of variational Gaussian process NARX models with GPGPU. *ISA Transactions* 109, 141-151, 2021.
- Luukkonen T., Modelling and control of quadcopter, Independent research project in applied mathematics Espoo, 1-26, 2011.
- Muliadi J., Kusumoputro B., Neural Network Control System of UAV Altitude Dynamics and Its Comparison with the PID Control System. *Journal of Advanced Transportation* 2018: 3823201, 1-18, 2018.
- Nguyen N.P., Mung N.X., Thanh H.L.N.N., Huynh T.T., Lam N.T., Hong S.K., Adaptive Sliding Mode Control for Attitude and Altitude System of a Quadcopter UAV via Neural Network, *IEEE Access* Volume: 9, 40076-40085, 2021.

- Paiva E., Soto J., Salinas J., Ipanaque W., Modeling, Simulation and Implementation of a modified PID Controller for stabilizing a Quadcopter, 2016 IEEE International Conference on Automatica (ICA-ACCA), 1-6, 2016.
- Praveen V., Pillai A. S., Modeling and Simulation of Quadcopter using PID Controller, IJCTA 9(15), 7151-7158, 2016.
- Razmi H., Afshinfar S., Neural network-based adaptive sliding mode control design for position and attitude control of a quadrotor UAV. Aerospace Science and Technology 91, 12-27, 2019.
- Wang P., Man Z., Cao Z., Zheng J., Dynamics Modelling and Linear Control of Quadcopter, International Conference on Advanced Mechatronic Systems 2016, 498-503, 2016.
- Yoon G.Y., Yamamoto A., Lim H.O., Mechanism and Neural Network Based on PID Control of Quadcopter, 16th International Conference on Control, Automation and Systems (ICCAS 2016), 19-24, 2016.
- Zulu A., John S., A review of control algorithms for autonomous quadrotors. Open Journal of Applied Sciences 4, 547-556, 2014.